A statistical study of the observed and modeled global thermosphere response to magnetic activity at middle and low latitudes

Chantal Lathuillère,[1] Michel Menvielle,[2,3] Aurélie Marchaudon,[4] and Sean Bruinsma[5]

Received 18 December 2007; revised 30 April 2008; accepted 19 May 2008; published 26 July 2008.

[1] From one year (2004) of thermosphere total density data inferred from CHAMP/STAR accelerometer measurements, we calculate the global thermosphere response to auroral magnetic activity forcing at middle and low latitudes using a method based on a singular value decomposition of the satellite data. This method allows separating the large-scale spatial variations in the density, mostly related to altitude/latitude variations and captured by the first singular component, from the time variations, down to timescales on the order of the orbital period, which are captured by the associated projection coefficient. This projection coefficient is used to define a disturbance coefficient that characterizes the global thermospheric density response to auroral forcing. For quiet to moderate magnetic activity levels ($Kp < 6$), we show that the disturbance coefficient is better correlated with the magnetic am indices than with the magnetic ap indices. The latter index is used in all empirical thermosphere models to quantify the auroral forcing. It is found that the NRLMSISE-00 model correctly estimates the main features of the thermosphere density response to geomagnetic activity, i.e., the morphology of Universal Time variations and the larger relative increase during nighttime than during daytime. However, it statistically underestimates the amplitude of the thermosphere density response by about 50%. This underestimation reaches 200% for specific disturbed periods. It is also found that the difference between daytime and nighttime responses to auroral forcing can statistically be explained by local differences in magnetic activity as described by the longitude sector magnetic indices.

Citation: Lathuillère, C., M. Menvielle, A. Marchaudon, and S. Bruinsma (2008), A statistical study of the observed and modeled global thermosphere response to magnetic activity at middle and low latitudes, *J. Geophys. Res.*, *113*, A07311, doi:10.1029/2007JA012991.

1. Introduction

[2] Since the launch of the CHAMP satellite in July 2000 at about 450 km altitude, in a near-circular orbit with an inclination of 87.3° [*Reigber et al.*, 2002], new measurements of the total mass density of the thermosphere are available, thanks to the high-precision STAR accelerometer. These measurements have been used to study the statistical properties of the thermosphere density global distribution [*Bruinsma et al.*, 2004; *Liu et al.*, 2005], and its response to geomagnetic activity forcing, in particular during severe geomagnetic storms [*Sutton et al.*, 2005; *Liu and Lühr*, 2005; *Forbes et al.*, 2005; *Bruinsma et al.*, 2006]. These studies underlined the inadequacy of semiempirical thermosphere models for correctly estimating the thermosphere density during storms at all latitudes. Such model inadequacy impacts geodetic products and orbital calculations as discussed by *Willis et al.* [2005].

[3] In a recent paper, *Guo et al.* [2007] focused on the effects of solar variability on CHAMP density measurements, using several solar proxies. They also assess the accuracy of empirical models in estimating the thermosphere response to variations induced by the solar rotation. The present paper is complementary. It aims at studying the relation between CHAMP densities and geomagnetic activity and at assessing the ability of the most recent version of the MSIS models (NRLMSISE-00) developed since the 1970s by *Hedin et al.* [1977] in accounting for geomagnetic forcing at low and middle latitudes. One full year of observations is analyzed in order to obtain statistically meaningful results.

[4] Two problems have to be solved to do such a statistical analysis: first, how to deal with the satellite altitude variation without using a model-dependent thermosphere scale height for data projection at a common altitude, and second, which density reference to use for quiet geomagnetic conditions.

[5] The method proposed by *Menvielle et al.* [2007] is based on a Singular Value Decomposition analysis (SVD) of CHAMP data on the one hand, and on a specific run of the

[1] Laboratoire de Planétologie de Grenoble, UJF, CNRS, Grenoble, France.
[2] Centre d'études des Environnements Terrestre et Planétaires, Université Versailles St-Quentin, CNRS, IPSL, Saint Maur, France.
[3] Département des Sciences de la Terre, Université Paris Sud, Orsay, France.
[4] Laboratoire de Physique et Chimie de l'Environnement, CNRS, Orléans, France.
[5] Department of Terrestrial and Planetary Geodesy, CNES, Toulouse, France.

0148-0227/08/2007JA012991

NRLMSISE-00 thermosphere model [*Picone et al.*, 2002] on the other hand. In this method, the analysis is limited to middle and low latitudes between 50°N and 50°S; the error in the observed densities due to residual winds (HWM93 [*Hedin et al.*, 1996] was used in the density derivation) is less than 10% and varies little with magnetic activity [*Sutton et al.*, 2007].

[6] During any 24-h UT interval (i.e., 15 orbits), the NS (respectively SN) orbit segments have almost the same local time (LT) and very similar latitude versus altitude profile. During periods of magnetic quietness, the density versus latitude profile is therefore expected not to change significantly from one orbit NS (respectively SN) segment to the next. These features strongly suggest that Singular Value Decomposition (SVD) is well suited to extract the altitude/latitude/LT reference profile from 24 h of data. Indeed, *Menvielle et al.* [2007] showed that such SVD analysis of orbit segments between 50°N and 50°S makes it possible to account for most of the density variation observed along one orbit segment in terms of a normalized profile (the first singular vector) multiplied by one projection coefficient, which has the dimension of a density. The latitude/altitude/LT dependence of large-scale density variations is taken into account by the normalized profile while the UT time dependence of the global thermosphere density behavior is taken into account by the projection coefficient.

[7] *Menvielle et al.* [2007] also showed that the NRLMSISE-00 thermosphere model can be used for obtaining a reference density when run with MgII indices [*Viereck et al.*, 2004], rescaled to F10.7 units, as a proxy of solar EUV radiations and a quiet magnetic activity diurnal Ap index equal to 4. They used this reference density to derive a thermosphere density disturbance coefficient, defined as the ratio of the CHAMP data projection coefficient to the projection coefficient calculated from the NRLMSISE-00 reference model. This disturbance coefficient can be considered as a proxy of the global response of thermosphere density to geomagnetic activity forcing for latitudes between 50°N and 50°S and in the range of CHAMP altitudes.

[8] In this paper, we have applied this method to CHAMP data of 2004. In the first part, after a quick reminder of the principle of this method, we present the disturbance coefficients obtained for August 2004 for both CHAMP and NRLMSISE-00 densities in detail. Then we compare the disturbance coefficients over the full year for the CHAMP densities and the modeled ones. In the second part of the paper, we determine by means of a statistical analysis how the disturbance coefficients vary with geomagnetic activity. We used both planetary and regional magnetic indices and discuss the differences between data and model. This enables us, in the last part, to assess the ability of NRLMSISE-00 to describe the density thermosphere response to magnetic activity at mid and low latitudes and for the low solar activity conditions that prevailed during the year 2004.

2. The 2004 Density Disturbance Coefficients

2.1. CHAMP Density Analysis

[9] The CHAMP density data used in this paper are the total density estimates derived from CHAMP/STAR accelerometer measurements sampled at 10 s intervals and interpolated to the nearest latitude degree value between 50°N and 50°S. The reduction of the CHAMP/STAR accelerometer data in terms of total density is described in detail by *Bruinsma et al.* [2004], and we refer the reader to this publication for an extensive description of the CHAMP density determination.

[10] A 15-orbit segment running SVD analysis is performed on consecutive intervals of data without gaps. We do not have results for the seven first and the seven last orbit segments of each time interval considered. We have therefore considered intervals of at least 3 days, leading to 15 time intervals for year 2004 ranging from 3 days to more than 1 month as the August interval shown below.

[11] For each orbit, the data are then projected on the first singular vector determined from the set of the considered orbit, the seven previous ones and the seven following ones. As explained by *Menvielle et al.* [2007], this projection captures the large-scale variations of the observed density along the satellite orbit segments. It is further illustrated in Figure 1, which displays the density and its projection along the daytime orbit segments, as a function of latitude and UT for August 2004. All the plots have the same color scale, displayed on the right of Figure 1. Note that altitude and latitude variations are combined in this color plot.

[12] The variations in the CHAMP densities are displayed in Figure 1 (top left). The densities are larger at middle latitudes in the Northern Hemisphere: this results from a combined effect of the satellite altitude variation and of the seasonal variation. A significant Universal Time (UT) dependence of the density for this month is clearly visible at all latitudes. This time variation includes the effects of both solar and magnetic activity. The low-density values observed during the first days of the month correspond to the magnetic quietness that prevails during this period. On the contrary, the higher-density values observed at northern midlatitudes during the subsequent period of 10–12 days correspond to the high solar activity and moderate magnetic activity observed during this period. The high density values observed at the end of the month over almost the whole latitude range correspond to the magnetic storm that occurred at that time: am peaks at 169 nT (and Kp at 7o) on 30 August, between 2100 and 2400 UT.

[13] Figure 1 (bottom left) displays the variations of the projection on the first singular vector. There is no significant difference between the original values (Figure 1, top) and their projections. Only during the storm at the end of the month, one can see that the smaller spatial scale variations, due to wave like perturbations, are smoothed out. This clearly illustrates the fact that more than 98% of the variance in the data is captured by their projection on the first principal component: the large-scale spatial variations in the density, mostly related to altitude/latitude variations are captured by the first singular vectors, which are normalized vectors, whereas the time variations of the thermosphere density at a global scale are captured by the associated projection coefficient C1, which has the dimension of a density. In the following we will focus on the variations of this projection coefficient. We associated with each projection coefficient value the UT of the equator crossing for the corresponding orbit segment. Therefore, we

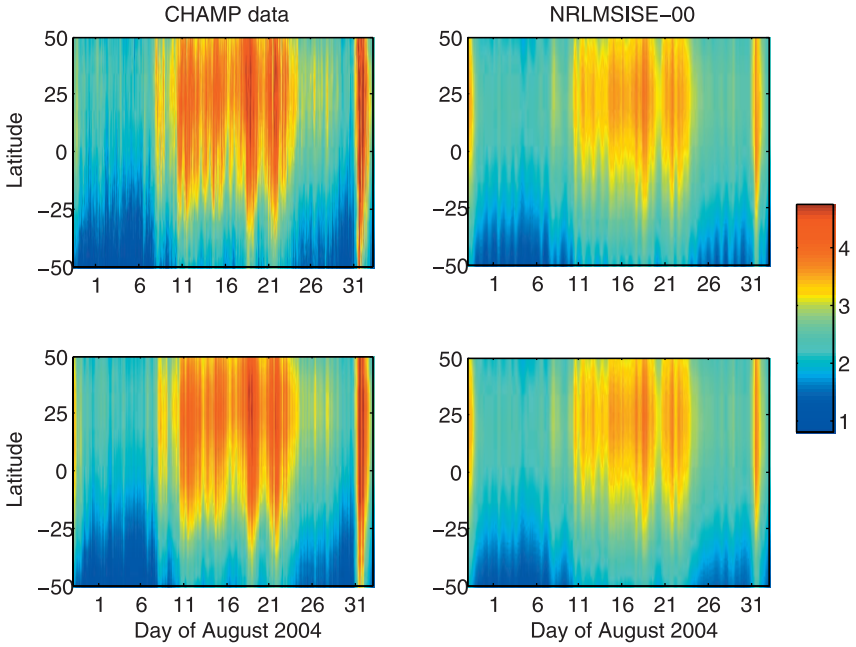

Figure 1. (top) CHAMP density estimates (left) and density computed by means of the NRLMSISE-00 actual model along the daytime NS orbit segments, as a function of latitude and UT during August 2004 (see text for the definition of the NRLMSISE-00 actual model). (bottom) Projection of the CHAMP density data (left) and NRLMSISE-00 computed density (right) on the first principal component (see text for further explanation). During August 2004 and along the NS orbit segments, LT at the satellite position varies from 1150 to 0845. For all cases, the density variations are displayed using the color scale displayed on the right; densities are expressed in terms of 10^{-12} kg m^{-3} units.

obtain one coefficient C1 every 92 min for NS (respectively SN) orbit segments.

2.2. NRLMSISE-00 Density Analysis

[14] Densities have also been calculated with the empirical NRLMSISE-00 model [*Picone et al.*, 2002] at the same location (altitude, latitude, longitude) and time as the CHAMP data, with two different sets of geomagnetic activity parameters: a first prediction used the model driven by the actual geomagnetic parameters ("actual model"), whereas a second prediction was obtained with a constant daily Ap of 4 ("reference model"). This procedure has already been used by *Lathuillère and Menvielle* [2004] in order to derive the thermospheric temperature perturbations due to magnetic activity.

[15] In the work of *Menvielle et al.* [2007], it is shown that using the Mg II index as a proxy for solar EUV instead of F10.7 in the NRLMSISE-00 model is more appropriate to account for the variations in the thermospheric density resulting from the solar EUV forcing at the solar rotation timescale. This is confirmed in the very recent study of *Guo et al.* [2007], who tested a variety of different solar flux indices over a 3 year period. *Guo et al.* [2007] also proposed to use the Seuv index [*Bowman and Tobiska*, 2006] as an alternative in the NRLMSISE-00 model to account for the solar rotation signal.

[16] In the present study, we use the composite MgII index [*Viereck et al.*, 2004] scaled to F10.7 (i.e., to sfu units, 1sfu = 10^{-22} W m^{-2} Hz^{-1}) using the linear relationship found between these two quantities over 42 months (January 2002 to June 2005). Our linear relation (MgII(sfu) = 7629*MgII-1953) is close to the relations provided by *Thuillier and Bruinsma* [2001] and *Bowman and Tobiska* [2006].

[17] The mean solar flux index used in our model runs is the 81 d centered average of scaled MgII values to which we added a constant of −5 sfu. This constant has been adjusted in a statistical way so that the CHAMP and model projection coefficients best agree over the full year during periods of very low magnetic activity. This adjustment accounts for any bias that could result from the CHAMP data reduction. It may also account for the fact that the model has not been constructed using the Mg II index. Let us stress that the value of this constant is representative of the thermosphere behavior for the year 2004 only, i.e., for a period of relatively low solar activity: another constant must be estimated when considering a different time period.

[18] The densities computed for August, using the NRLMSISE-00 actual model predictions, are displayed in Figure 1 (top right). Their projections on the first singular vector are displayed in Figure 1 (bottom right). They are identical to the original model values. This is not surprising since small-scale spatial and time variations, e.g., gravity waves, are smoothed out in the course of the statistical derivation of empirical models from high-resolution data sets.

[19] Comparison of modeled with observed densities shows that they have a similar behavior: maximum at northern midlatitudes, with low values during the first days of the month, then higher values for about a 10-day period,

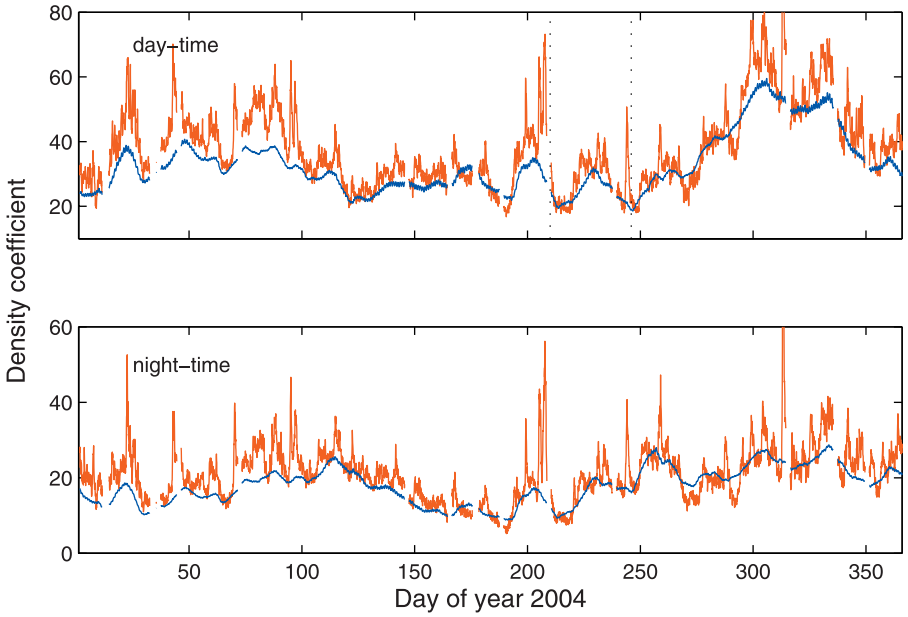

Figure 2. Variations with UT over the year 2004 of the projection coefficients for the densities estimated from the CHAMP observations (red lines) and for those computed using the reference NRLMSISE-00 model (blue lines; see text for the definition of the NRLMSISE-00 reference model). (top) Daytime orbit segments and (bottom) nighttime orbit segments.

and a significant increase in density values at the end of the month. However, the modeled densities are significantly smaller than the observed ones during periods of magnetic activity. Furthermore, the response of the density model to geomagnetic activity forcing is relatively similar in amplitude during the period of moderate magnetic activity in the middle of the month and during the storm that occurred at the end of the month, while the observations reveal that this is clearly not the case. This is an illustration of the well-known underestimation by empirical models of the thermosphere density response to the magnetic activity forcing.

2.3. The Density Disturbance Coefficients for Year 2004

[20] As already stated in the introduction, *Menvielle et al.* [2007] introduced the CHAMP disturbance coefficient Cd, defined as the ratio of the observed CHAMP density projection coefficient C1 to the reference model one C1ref. These authors also introduced the model disturbance coefficient Cdm = C1m/C1ref, where C1m is the actual model density projection coefficient. The actual and reference models were described in the previous section.

[21] Now we focus on the variations of these disturbance coefficients and of their relative variations with UT. Remember that one coefficient is obtained for each descending and ascending part of the CHAMP orbit, i.e., every 92 min, and characterizes the low-latitude to midlatitude densities (50°N to 50°S).

[22] Figure 2 shows the variations of the projection coefficients for the CHAMP data (red line) and for the densities computed with the reference model (blue line) over the whole year 2004. Figure 2 (top) corresponds to daytime orbit segments (i.e., 8 h < LT < 20 h), and Figure 2 (bottom) corresponds to nighttime orbit segments. The local time limits between daytime and nighttime have been determined from the data: they correspond to similar density coefficients for the descending and ascending part of the orbit. The blue curve corresponds to the reference situation defined, as explained above, as the thermosphere density behavior in absence of magnetic activity and hereafter denoted as reference projection coefficient. Note that during some periods the red curve is slightly below the blue one (e.g., around days 190, 270, and 290) i.e., the CHAMP projection coefficient is smaller than the reference one. Remember that the adjustment of model parameters has been made on a statistical basis, which may explain such situations.

[23] The long-term variations of the reference projection coefficient correspond to the response of the thermosphere density at the CHAMP orbit to its forcing by the solar radiations apart from solar flare periods: they capture UT, LT and seasonal variations as well as the altitude effect associated to the decrease (of about 20 km) of the mean satellite altitude over the year. One can note that the projection coefficients are significantly larger during daytime than during nighttime, reflecting the diurnal variation of the thermosphere total density, and that the difference between the CHAMP projection coefficient (red curve) and the reference one (blue curve) is highly variable.

[24] Figure 3 presents the variations of the CHAMP disturbance coefficients Cd during 2004 (red curves) for daytime and nighttime (Figure 3, top and middle), respectively. As expected, this coefficient no longer has long-term variations related to the thermosphere forcing by the solar radiation. Figure 3 also shows the already evidenced [see *Menvielle et al.*, 2007] high correlation between the thermosphere relative density variations and the geomagnetic activity described by the ap index (Figure 3, bottom).

[25] The variations of the model disturbance coefficients Cdm are also plotted on Figure 3 (black curve; Figure 3, top

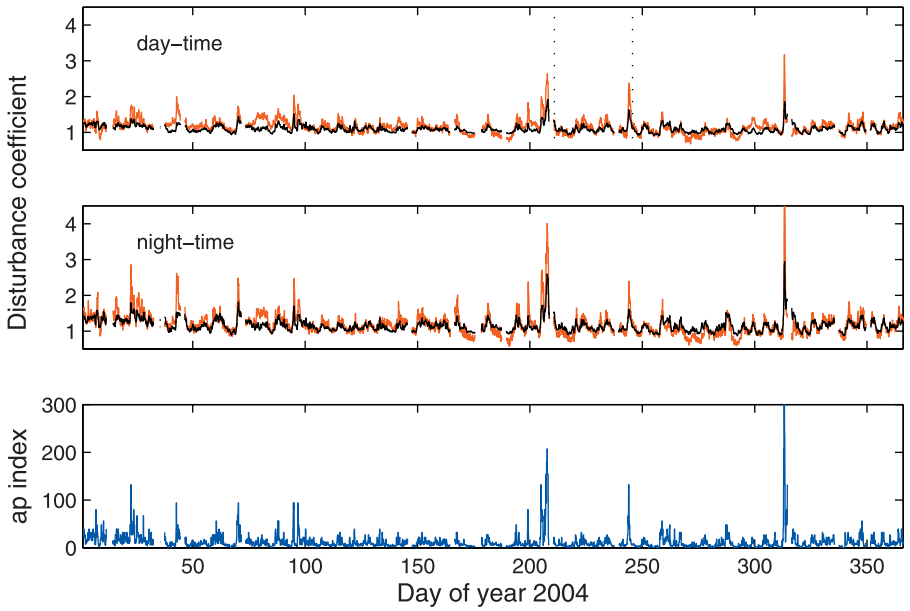

Figure 3. Variations with UT over the year 2004 of the CHAMP (red line) and NRLMSISE-00 (black line) density disturbance coefficients for (top) daytime and (middle) nighttime. (bottom) The variations of the ap magnetic activity index (in ap unit, i.e., ∼2nT).

and middle). The time variations of the CHAMP and model disturbance coefficients are very similar. This gives a striking confirmation that the NRLMSISE-00 model provides a good description of the phase of the thermosphere density response to the solar wind-forcing. The model disturbance coefficient is, however, always smaller than the CHAMP one, except of course during the already mentioned time intervals for which the CHAMP disturbance coefficient is smaller than 1. This shows that the underestimation by empirical models of the thermosphere density response observed during large storms is also present during periods of moderate magnetic activity forcing.

3. Statistical Analysis of the Global Density Disturbances

3.1. Use of Planetary Geomagnetic Indices

[26] In order to get a quantitative description of the thermosphere density forcing by geomagnetic activity, we binned the CHAMP and model disturbance coefficients (Cd and Cdm) as a function of geomagnetic activity at a planetary scale. We used the two geomagnetic indices ap (or Kp) and am (or Km) derived from two different observatory networks at subauroral latitudes [*Menvielle and Berthelier*, 1991; *Menvielle and Marchaudon*, 2007].

[27] The time delay between the energy deposition in the auroral ionosphere and the main thermosphere response at mid and low latitudes is generally estimated in the range 3 to 6 h [*Hedin et al.*, 1981]; we used the planetary geomagnetic indices with a constant delay of 3 h.

[28] Figure 4 presents the results obtained for the CHAMP (Figure 4, left) and model (Figure 4, right) disturbance coefficients for nighttime (black) and daytime (red) orbit segments. The disturbance coefficients are binned in terms of ap values (Figure 4, top) and of am values (Figure 4, bottom). Note that the scales of the horizontal axes are different to take into account the difference between ap and am units (∼2 nT and 1 nT, respectively; see *Menvielle and Berthelier* [1991] for further explanations). The error bars correspond to 95% confidence intervals of the expected value determination, assuming a Student statistical distribution of the data. We rejected bins with less than 20 values and therefore restrict this statistical analysis to a magnetic activity level of Kp smaller than 6 (ap < 60 and am < 120 nT).

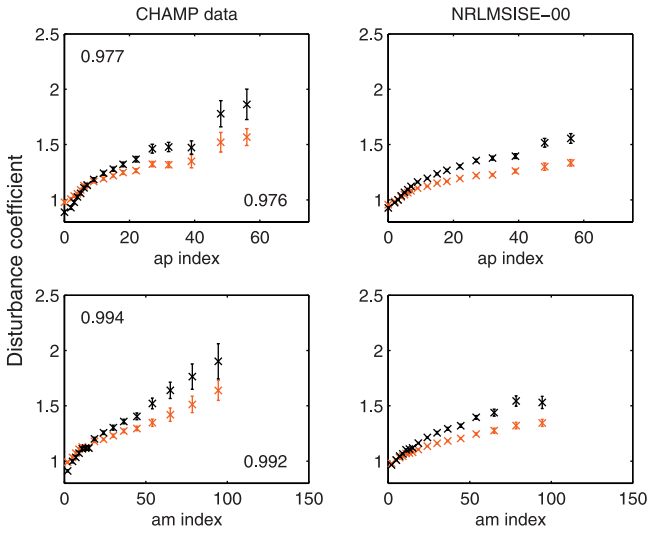

Figure 4. Binning of the (left) CHAMP and (right) model disturbance coefficients as a function of geomagnetic activity at a planetary scale, as characterized by the planetary geomagnetic indices (top) ap and (bottom) am, delayed by 3 hours. The ap values are expressed in ap unit (i.e., ∼2 nT) while am values are expressed in nT. Nighttime results are plotted in black and daytime results are in red.

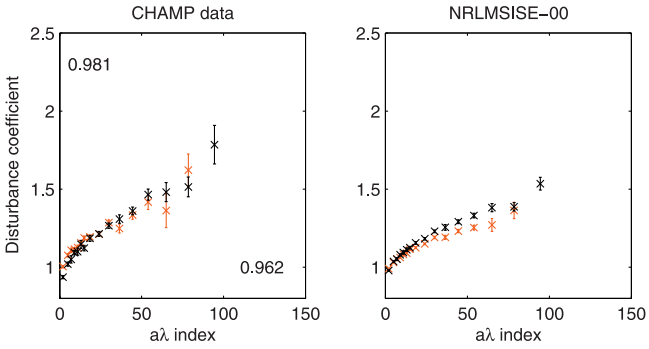

Figure 5. Binning of the (left) CHAMP and (right) model disturbance coefficients as a function of geomagnetic activity characterized at a regional scale by the longitude sector geomagnetic indices aλ delayed by three hours. Nighttime results are plotted in black and daytime results are in red. The aλ unit is nT.

[29] Figure 4 shows the increase of nighttime and daytime disturbance coefficients with planetary magnetic indices. This increase is larger for CHAMP data than for the model as already mentioned. Note that both the CHAMP and model disturbance coefficient increases are larger during nighttime than during daytime. For CHAMP data, this increase is about 90% during night and 60% during day for am ~100 nT (i.e., Kp ~ 5+). The correlation coefficients between CHAMP data and magnetic indices are indicated on the plot respectively for day time and nighttime, in the lower right and upper left corners. They are significantly higher when the binning is done with am indices than when the binning is done with ap indices. Figure 4 clearly suggests using am indices in the case of the CHAMP coefficients. This is not surprising, since the am index gives a better estimation of the geomagnetic activity at a planetary scale, thanks to the better longitude distribution of the observatories that make up its network [see, e.g., *Menvielle and Berthelier*, 1991; *Menvielle and Marchaudon*, 2007].

3.2. Use of Longitude Sector Indices

[30] The spatial distribution of the thermosphere heating sources associated to geomagnetic activity, mostly related to Joule heating and particle precipitation, are extremely variable [*Shue et al.*, 2001; *Mcharg et al.*, 2005, and references therein]. It is therefore expected that accounting of the geomagnetic activity effect on global thermosphere density by means of planetary magnetic indices, which is actually done in the semiempirical atmospheric models, does not result in an accurate description of the upper thermosphere disturbance (see Figures 3 and 4). This suggests characterizing the spatial dependence of the geomagnetic activity by means of the 3-h longitude sector indices proposed by *Menvielle and Paris* [2001]. Indeed, *Lathuillère and Menvielle* [2004] already showed that the use of these regional indices allowed a better characterization of thermospheric temperature perturbation derived from UARS/WINDII observations, than the usual planetary indices.

[31] Figure 5 shows the CHAMP (Figure 5, left) and model (Figure 5, right) disturbance coefficients binned in terms of longitude sector indices, for both daytime (red) and nighttime (black) data. The most striking feature of this plot is the almost complete overlap of day and night results for CHAMP. The increase of CHAMP disturbance coefficients with regional indices is the same for night and day. This means that, statistically speaking and for the low solar activity conditions of year 2004, the relative increase of the thermosphere density with magnetic activity does not depend on the thermosphere background condition, which is primarily dependent on the solar EUV heating. This also implies that the regional indices during nighttime are statistically larger than during daytime.

[32] We have verified this latter statement by doing a statistical analysis of the longitude sector indices as a function of local time. Results are shown on Figure 6. For different levels of geomagnetic activity (represented by different colors), the mean values of the longitude sector indices are plotted over 20 years (1985–2005) as a function of 3 h LT intervals. For the sake of clarity, values corresponding to Km = 3 (i.e., Kp ~ 3) have been linked by a black line and values corresponding to Km = 6 (i.e., Kp ~ 6) by a purple line. Regardless of the level of magnetic activity, it is almost twice smaller in the 0900–1200 LT interval than in 1800–0300 LT interval.

[33] The correlation coefficient between CHAMP data and regional indices are indicated on Figure 5 respectively for daytime and nighttime, in the lower right and upper left corners. They are significantly lower than those computed using planetary am indices, which may result from the fact that the variability is larger for regional indices than for am planetary indices.

[34] In terms of difference between daytime and nighttime, the model disturbance coefficients have the same behavior as the CHAMP ones: when using planetary indices, the relative difference between daytime and nighttime has the same magnitude for CHAMP (Figure 4, left) and model coefficients (Figure 4, right). When longitude sector indices are used, the difference between daytime and nighttime model disturbance coefficients becomes very

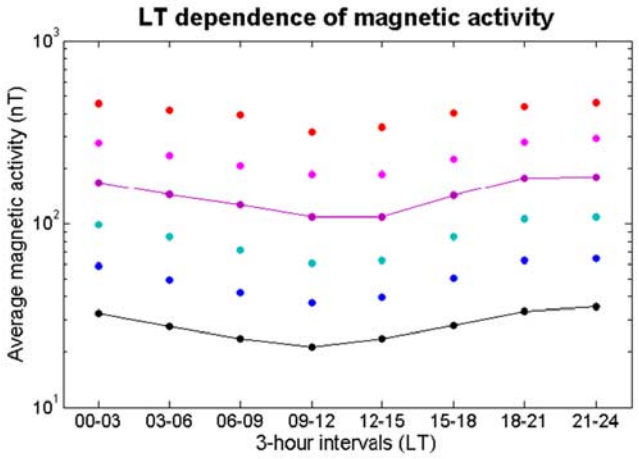

Figure 6. Mean LT dependence of the regional geomagnetic activity for different levels of the planetary magnetic activity calculated over 1985–2005. Each color corresponds to a different activity level from Km = 3 (black) to Km = 8 (orange) in steps of 1.

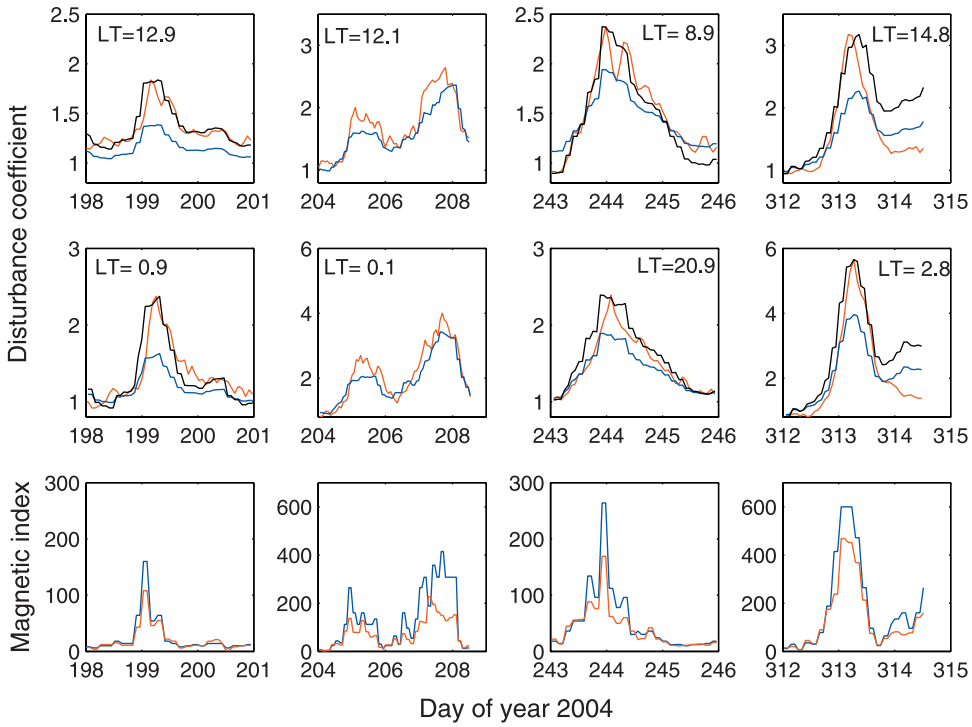

Figure 7. Zoom of selected storms in our data set for which the global relative density increase during nighttime is larger than 100% (disturbance coefficient > 2). (top) Daytime and (middle) nighttime data are plotted and local time is indicated. The red and blue lines show the CHAMP and the adjusted model disturbance coefficients, respectively. In black, the model disturbance coefficient has been normalized to the CHAMP one in order to highlight the similarity of their UT morphology. (bottom) Planetary ap (in ap unit) and am indices (in nT unit) are plotted in blue and black lines, respectively, using a scale factor two times larger for ap than for am: since 1 ap unit ~2 nT, the curves corresponding to ap indices and to am indices are expected to be similar.

small (Figure 5, right). Implications for model characteristics are discussed next.

4. An Assessment of the NRLMSISE-00 Model

[35] The disturbance coefficients are underestimated by NRLMSISE-00 as shown in Figures 4 and 5, regardless of the magnetic indices used to bin the data. However, the model characterization presented in section 3.1 may be challenged since the binning was done using the magnetic index from the previous 3 h time interval only, whereas the NRLMSISE-00 model requires a full history of magnetic activity over 33 h prior to the current time. In order to quantify this underestimation, let us consider data that were not binned.

[36] The linear correlation coefficient, calculated with 5300 daytime values (of year 2004), is 0.76 and the model underestimates the CHAMP disturbances by 46%. For nighttime, the correlation coefficient is 0.85 and the underestimation is equal to 55%. This underestimation is mainly valid when Kp is less than 6 because we have very few values for larger magnetic activity.

[37] In order to assess the behavior of the model during the most disturbed periods, we have selected events on the basis of the maximum value reached by the density disturbance coefficient during periods of magnetic activity. During year 2004, nine events correspond to a global thermosphere density increase of more than 100% (disturbance coefficient > 2) during nighttime (see Figure 3). In Figure 7, CHAMP and model disturbance coefficients are compared for four selected periods: a relatively small storm on 17 July (day 199), the two contiguous storms of 23 and 25 July (days 205 and 207), the storm of 31 August displayed in Figure 1 (day 244), and finally the intense storm on 8 November.

[38] Figure 7 (top and middle) displays the CHAMP disturbance coefficient (red curves) and the model disturbance coefficient that has been adjusted by the 46% or 55% statistical underestimation (blue curve), for daytime and nighttime, respectively. The adjusted model disturbance coefficients have the same morphology of UT variations as the CHAMP ones for all storms, and comparable amplitudes for the two storms in July (day 205 and 207). For the other three selected events the statistical correction is still much too small, whatever the magnetic activity level

[39] For these three storms, we have added a black curve to the plots that corresponds to a normalization of the amplitude of the variation of the model disturbance coefficient to CHAMP one. The normalization is done independently for the three storms and for daytime and nighttime. These new curves confirm that the morphology of UT variations during the disturbed periods is very well predicted by the model in spite of the amplitude underestimation. This underestimation, which has the same order of

magnitude for daytime and nighttime, varies between about 150% for August and November storms and 220% for the worst case of July 17.

[40] A slight phase difference can also be noticed on several days, with an increase of the predicted density earlier than the observed one (day 199, daytime and nighttime; day 243 and 312, nighttime). A detailed study of phase differences between thermosphere responses to magnetic storms and their model predictions would require a higher time resolution in the description of geomagnetic activity, presently limited to three hours. This question will be addressed in a future study.

[41] Figure 7 (bottom) displays the planetary ap indices which drive the model and the planetary am indices using a scale factor two times larger for ap than for am: since 1 ap unit $\sim$2 nT, the curves corresponding to ap indices (blue lines) and to am indices (red lines) are expected to be similar. It is the case during periods of moderate magnetic activity but not during periods of intense geomagnetic activity where the curves can be very different, the am curve being always significantly below the ap one. The choice of ap indices for describing magnetic activity in the model may explain part of the variability of the error in the model amplitude estimation. However, one should also stress that the storm observed on 17 July, for which the model underestimation is the largest, corresponds to the period with the smallest magnetic indices.

[42] Finally, note that during the storm of 31 August, when CHAMP was in the dawn-dusk plane, the relative density increase has almost the same amplitude on either side of the Earth but occurs later in the dusk sector. This phase difference will be addressed in the future using a geomagnetic activity indicator with a time resolution higher than 3 h.

5. Summary

[43] Using 1 year of total density estimates around 400 km altitude, we have made a statistical analysis of the global response of the middle to low latitude thermosphere to auroral energy inputs. In opposition to what is usually done, our method does not involve any a priori information on the atmosphere scale height to get rid of the satellite altitude variations. It uses a reference model to describe the state of the thermosphere in absence of magnetic activity. The density disturbance coefficient that we obtained describes the large scale expansion of the thermosphere in response to the solar wind-magnetosphere-ionosphere-thermosphere coupling processes.

[44] We showed that the disturbance coefficient is better correlated with the magnetic am indices than with ap, which is currently in use in all empirical thermosphere models. The relative increase of density with planetary indices is larger during nighttime than during daytime, the order of magnitude being 90% during night and 60% during day for am $\sim$100 nT (i.e., Kp $\sim$ 5+).

[45] We have also shown that this day/night discrepancy disappears when one uses longitude sector magnetic indices, which may therefore serve as a proxy to monitor the local time dependence of the thermosphere disturbance coefficient for magnetic activity levels less than Kp $\sim$ 6. In fact, the relative density increase with magnetic activity appears to be independent on the background thermospheric conditions, which are different during day and night. Note that this result has been obtained for low solar activity conditions, and that it has to be assessed for high solar activity conditions, when nighttime and daytime densities differ much more.

[46] The disturbance coefficient has also been calculated using NRLMSISE-00 predicted densities along the CHAMP orbits. This allowed us to assess the validity of the model to describe the response of the thermosphere to magnetic activity during low solar activity conditions at low and middle latitudes. We found that the model statistically underestimates the density disturbance by about 50% for magnetic activity levels less than Kp $\sim$ 6 and correctly reproduces the statistical day/night difference.

[47] During more disturbed periods, we have found that the model can underestimate the density disturbance amplitude by more than 200%, while it correctly reproduced the morphology of the UT variations of the density disturbance. In some cases, we have also detected a slight phase shift with an increase of predicted densities earlier than observed ones. Further studies of such phase differences will be done using magnetic indices with improved time resolution.

[48] We think that this study will help provide insight for improving the thermosphere modeling capacity. Using am indices or longitude sector indices to construct the models may allow obtaining a more accurate quantitative description of the large-scale expansion of the thermosphere resulting from space weather events.

[49] **Acknowledgments.** CHAMP is managed by GFZ, Potsdam, Germany. The STAR accelerometer was provided by CNES, Toulouse, France. This research has been supported by the French CNRS/INSU Programme National Soleil-Terre. The authors thank Rodney Viereck for providing the composite MgII index data series used in this paper.

[50] Zuyin Pu thanks Denis Alcayde and another reviewer for their assistance in evaluating this paper.

References

Bowman, B. R., and W. K. Tobiska (2006), Improvements in modelling thermospheric densities using new EUV and FUV solar indices, paper presented at 16th AAS/AIAA Space Flight Mechanics Meeting, Am. Astron. Soc., Tampa, Fla.

Bruinsma, S., D. Tamagan, and R. Biancale (2004), Atmospheric densities derived from CHAMP/STAR accelerometer observation, *Planet. Space Sci.*, *52*, 297–312, doi:10.1016/j.pss.2003.11.004.

Bruinsma, S., J. M. Forbes, R. S. Nerem, and X. Zhang (2006), Thermosphere density response to the 20–21 November, 2003 solar and geomagnetic storm from CHAMP and GRACE accelerometer data, *J. Geophys. Res.*, *111*, A06303, doi:10.1029/2005JA011284.

Forbes, J. M., G. Lu, S. Bruinsma, R. S. Nerem, and X. Zhang (2005), Thermosphere density variation due to the April 15–24, 2002 solar event from CHAMP/STAR accelerometer measurements, *J. Geophys. Res.*, *110*, A12S27, doi:10.1029/2004JA010856.

Guo, J., W. Wan, J. M. Forbes, E. Sutton, R. S. Nerem, T. N. Woods, S. Bruinsma, and L. Liu (2007), Effects of solar variability on thermosphere density from CHAMP accelerometer data, *J. Geophys. Res.*, *112*, A10308, doi:10.1029/2007JA012409.

Hedin, A. E., et al. (1977), A global thermospheric model based on mass spectrometer and incoherent scatter radar data, MSIS 1, N2 density and temperature, *J. Geophys. Res.*, *82*, 2148–2156, doi:10.1029/JA082i016p02148.

Hedin, A. E., N. W. Spencer, H. G. Mayr, and H. S. Porter (1981), Semi-empirical modeling of thermospheric magnetic storms, *J. Geophys. Res.*, *86*, 3515–3518, doi:10.1029/JA086iA05p03515.

Hedin, A. E., et al. (1996), Empirical wind model for the upper, middle, and lower atmosphere, *J. Atmos. Terr. Phys.*, *58*, 1421–1447, doi:10.1016/0021-9169(95)00122-0.

Lathuillère, C., and M. Menvielle (2004), WINDII thermosphere temperature perturbation for magnetically active situations, *J. Geophys. Res.*, *109*, A11304, doi:10.1029/2004JA010526.

Liu, H., and H. Lühr (2005), Stong disturbance of the upper thermospheric density due to magnetic storms: CHAMP observations, *J. Geophys. Res.*, *110*, A09S29, doi:10.1029/2004JA010908.

Liu, H., H. Lühr, V. Henize, and W. Köhler (2005), Global distribution of the thermospheric total mass density derived from CHAMP, *J. Geophys. Res.*, *110*, A04301, doi:10.1029/2004JA010741.

Mcharg, M., F. Chun, D. Knipp, G. Lu, B. Emery, and A. Ridley (2005), High latitude joule heating response to IMF inputs, *J. Geophys. Res.*, *110*, A08309, doi:10.1029/2004JA010949.

Menvielle, M., and A. Berthelier (1991), The K-derived planetary indices: Description and availability, *Rev. Geophys. Space Phys.*, *29*, 415–432. (Correction, *Rev. Geophys. Space Phys.*, *30*, 91, doi:10.1029/92RG00461, 1992.)

Menvielle, M., and A. Marchaudon (2007), Geomagnetic indices in solar-terrestrial physics and space weather, in *Space Weather: Research Toward Applications in Europe*, edited by J. Lilensten, pp. 277–288, Springer, New York.

Menvielle, M., and J. Paris (2001), The aλ longitude sector geomagnetic indices, *Contrib. Geophys. Geod.*, *31*, 315–322.

Menvielle, M., C. Lathuillère, S. Bruinsma, and R. Viereck (2007), A new method for studying the thermosphere density variability derived from CHAMP/STAR accelerometer data for magnetically active conditions, *Ann. Geophys.*, *25*, 1949–1958, SRef-ID:1432-0576/angeo/2007-25-1949.

Picone, J. M., A. E. Hedin, D. P. Drob, and A. C. Aikin (2002), NRLMSISE-00 empirical model of the atmosphere: Statistical comparisons and scientific issues, *J. Geophys. Res.*, *107*(A12), 1468, doi:10.1029/2002JA009430.

Reigber, C., H. Lühr, and P. Schwintzer (2002), CHAMP mission status, *Adv. Space Res.*, *30*, 129–134, doi:10.1016/S0273-1177(02)00276-4.

Shue, J. H., P. T. Newell, K. Liou, and M. C. Meng (2001), Influence of interplanetary magnetic field on global auroral patterns, *J. Geophys. Res.*, *106*, 5913–5926, doi:10.1029/2000JA003010.

Sutton, E. K., J. M. Forbes, and R. S. Nerem (2005), Global thermospheric neutral density and wind response to the severe 2003 geomagnetic storms from CHAMP accelerometer data, *J. Geophys. Res.*, *110*, A09S40, doi:10.1029/2004JA010985.

Sutton, E. K., R. S. Nerem, and J. M. Forbes (2007), Density and winds in the thermosphere deduced from accelerometer data, *J. Spacecr. Rockets*, *44*, 1210–1219, doi:10.2514/1.28641.

Thuillier, G., and S. Bruinsma (2001), the Mg II index for upper atmosphere modelling, *Ann. Geophys.*, *19*, 219–228.

Viereck, R. A., L. E. Floyd, P. C. Crane, T. N. Woods, B. G. Knapp, G. Rottman, M. Weber, L. C. Puga, and M. T. Deland (2004), A composite Mg II index spanning from 1978 to 2003, *Space Weather*, *2*, S10005, doi:10.1029/2004SW000084.

Willis, P., F. Deleflie, F. Barlier, Y. E. Bar-Sever, and L. J. Romans (2005), Effects of the thermosphere total density perturbation on LEO orbits during severe geomagnetic conditions (Oct–Nov 2003) using DORIS and SLR data, *Adv. Space Res.*, *36*, 522–533, doi:10.1016/j.asr.2005.03.029.

S. Bruinsma, Department of Terrestrial and Planetary Geodesy, CNES, F-31401 Toulouse Cedex 4, France.

C. Lathuillère, Laboratoire de Planétologie de Grenoble, UJF, CNRS, BP 53, F-38041 Grenoble Cedex, France.

A. Marchaudon, Laboratoire de Physique et Chimie de l'Environnement, CNRS, F-45071 Orléans Cedex 2, France.

M. Menvielle, Centre d'études des Environnements Terrestre et Planétaires, Université Versailles St-Quentin, CNRS, IPSL, F-94107 Saint Maur Cedex, France.